Fisher, A., Davis, E.E., and Escutia, C. (Eds.), 2000
Proceedings of the Ocean Drilling Program, Scientific Results, Vol. 168

4. CALCAREOUS NANNOFOSSILS FROM LEG 168: BIOCHRONOLOGY AND DIAGENESIS[1]

X. Su,[2,3] K.-H. Baumann,[4] and J. Thiede[2]

ABSTRACT

A study on late Pliocene and Quaternary calcareous nannofossils from the eastern flank of the Juan de Fuca Ridge was carried out to provide a detailed biochronology for sediments recovered during Leg 168 and to investigate the effects of hydrothermal circulation and turbidite activity on diagenesis of nannofossils.

Through high-resolution stratigraphical analysis, 10 Quaternary nannofossil events were determined and a detailed biochronology of the Quaternary was obtained. Upper Pliocene sediments were also recovered but did not contain any upper Pliocene marker species, such as *Discoaster* species. However, an age of younger than 3.2 Ma was estimated for these sediments based on evidences of nannofossil assemblages.

Based on the resolved biostratigraphy, sedimentation rates of sediment sequences at these 10 sites and their variations were determined. A sedimentation hiatus between basal sediments and basements in this young seafloor region was observed.

Relative abundance of nannofossils in sediments is largely changed by dilution of turbiditic materials. Evidence suggests that variations in relative group abundance of nannofossils in the Juan de Fuca Ridge, affected by dilution of turbiditic materials, does not reflect the real variation in production of this group of microfossils.

Observations of this study suggest that calcite overgrowth of nannofossils is controlled by temperature, heat flow, thermal gradient in sediments, and the variation in composition of pore water, as well as the supply of calcite materials in sediments. These results provide a detailed knowledge about effects of low-temperature hydrothermal alteration on diagenesis of nannofossils.

Downhole variations in dissolution degree of nannofossils in sediment sequences at all Leg 168 sites were presented and compared with pH profiles. The correlation between these data indicates that nannofossils are very sensitive to variations in pH units in sediments. A reduction of pH will result in dissolution of nannofossils. Variations in pH units are induced by hydrothermal circulation as a result of a number of interactions between water/sediments and water/basement. The dissolution of nannofossils at Sites 1031 and 1032 were directly affected further by the pore-water upward flows at these two sites.

A few records of nannofossil preservation suggest that the effects of hydrothermal activity on diagenesis of nannofossils might involve more complicated processes and mechanisms that we do not understand yet.

INTRODUCTION

The Juan de Fuca Ridge is a seafloor spreading center lying 300–400 km off the coast of North America (Vine and Wilson, 1995). Hydrothermal activity in the region has been observed (Baker et al., 1987; Davis and Fisher, 1994; Ginster et al., 1994). The eastern flank of the Juan de Fuca Ridge is covered by upper Pliocene and Quaternary sediments. These sediments seal and host hydrothermal fluid flow, confining fluids in the crust at high average temperatures and leading to hydrothermal alteration of minerals in sediments (Lister, 1970; Davis et al., 1992; Davis, Mottl, Fisher, et al., 1992; Davis and Currie, 1993; Davis and Fisher, 1994).

The objective of Leg 168 was to study several common hydrothermal regimes that occur on the eastern flank of the Juan de Fuca Ridge (Davis, Fisher, Firth, et al., 1997). During Leg 168, 12 holes at 10 sites were drilled along a transect spanning oceanic crustal ages from 0.6 to 3.6 Ma with sediment thicknesses varying from 50 to 620 m (Table 1; Figs. 1–3). These sediments contain calcareous nannofossils with a variety of abundance and preservation states.

Previous studies of calcareous nannofossils from the high latitudes of the northeast Pacific dealt with nannofossil zonations (Gartner, 1970; Bukry and Bramlette, 1970; Bukry, 1971a, 1971b, 1973, 1981; Haq and Lipps, 1971; Hay, 1971; Wise, 1973; Worsley, 1973). Mao and Wise (1994) studied calcareous nannofossils from the Middle Valley of the Juan de Fuca Ridge and determined two upper Quaternary biostratigraphic zonations for sediment sequences of Leg 139.

Very few previous studies dealt with diagenesis of nannofossils subjected to hydrothermal activity. Mao and Wise (1994) first observed that nannofossils were strongly dissolved due to hydrothermal activity when high temperatures ranged from about 65° to higher than 200°C. In the area of Leg 168, on the eastern flank of the Juan de Fuca Ridge, basement temperatures are low, varying from 15° to 62°C (Davis, Fisher, Firth, et al., 1997). Leg 168 materials allow us to investigate the effect of low-temperature hydrothermal alteration on diagenesis of nannofossils.

Sediments from the eastern flank of the Juan de Fuca Ridge are dominated by turbiditic depositions. The effects of turbidites on the postdepositional preservation of nannofossils should be considered and examined.

For the reasons above, the nominal objective of this study is to provide a detailed biochronology for Pliocene and Quaternary sediments of Leg 168. Another aim of this study is to investigate the effects of hydrothermal circulation and turbidite activity on the postdepositional variations of nannofossils.

MATERIALS AND METHODS

Materials

The sediment region on the eastern flank of the Juan de Fuca Ridge belongs to the Cascadia Basin off the coast of North America.

[1]Fisher, A., Davis, E.E., and Escutia, C. (Eds.), 2000. *Proc. ODP, Sci. Results,* 168: College Station TX (Ocean Drilling Program).

[2]GEOMAR Research Centre for Marine Geosciences, Wischhofstraße 1-3, D-24148 Kiel, Germany.

[3]Present address: China University of Geosciences, 29 Xueyuan Road, Beijing 100083, Peoples Republic of China. xsu@cugb.edu.cn

[4]FB Geowissenschaften, Universität Bremen, Postfach 330440, D-28334 Bremen, Germany.

Table 1. Summary of Leg 168 sites and samples investigated.

Site	Hole	Latitude	Longitude (mbsl)	Water depth (mbsl)	Depth (mbsf)	Age of basement (Ma)	Number of samples analyzed
1023	A	47°55.040′N	128°47.529′W	2600	192.8	0.86	130
1024	B	47°54.274′N	128°45.132′W	2637	167.8	0.97	80
1025	B	47°54.998′N	128°39.052′W	2637	97.5	1.24	45
1026	A+C	47°46.261′N	127°45.186′W	2638	228.9	3.52	76
1027	B+C	47°45.387′N	127°43.867′W	2679	613.8	3.58	170
1028	A	47°51.479′N	128°30.289′W	2659	132.5	1.62	66
1029	A	47°49.901′N	128°22.597′W	2653	220.1	1.95	115
1030	B	47°53.847′N	128°33.711′W	2574	46.9	1.43	24
1031	A	47°53.400′N	128°33.970′W	2588	41.3	1.43	68
1032	A	47°46.773′N	128°07.341′W	2644	290.3	2.62	135

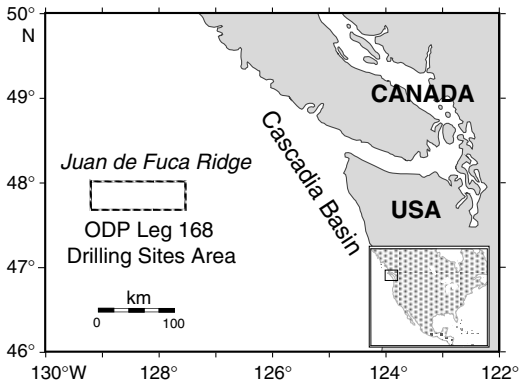

Figure 1. Locations of Leg 168 sites in the northeast Pacific.

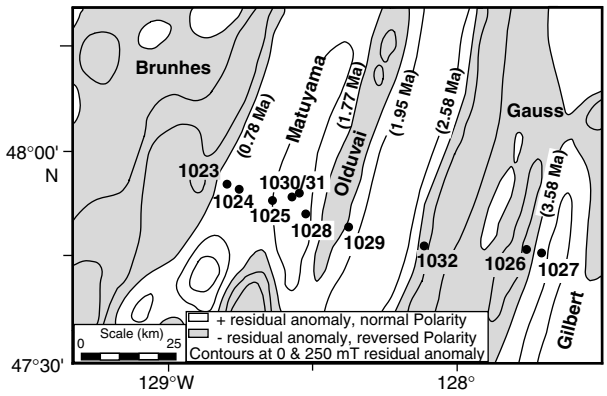

Figure 2. Leg 168 sites drilled on the eastern flank of the Juan de Fuca Ridge.

Quaternary sediments were obtained from all Leg 168 sites. Lithostratigraphically, they are mainly composed of thin-bedded turbidites (silt to sandy silt), thick-bedded sandy turbidites, and/or hemipelagic mud. These turbidite sediments are supplied from Pleistocene glacial sources along the continental margin. Upper Pliocene sediments were recovered only at Site 1027 and are characterized by hemipelagic mud and carbonate-rich mud (Davis, Fisher, Firth, et al., 1997).

We examined 804 nannofossil samples from 12 holes at the 10 sites (Table 1). These samples span, commonly, 20–150 cm of depth in core and were usually carefully selected from hemipelagic mud layers where nannofossils are common to abundant. However, samples from long sequences of thin-bedded turbidites were also taken to obtain enough time resolution. In these samples, nannofossils are rare or barren.

Generally, nannofossils of Leg 168 are well preserved in most sediments. Nannofossil age assignments were based mainly on samples in which nannofossils are well preserved.

Methods

Smear slides were prepared using standard techniques. For species analyses, relative counts were made and nannofossils were examined by means of a light microscope (LM) at 1200× to 2000× magnifications. Most Quaternary nannofossil species are too small to be identified accurately using LM; thus a number of samples were selected to ensure determination by means of scanning electron microscope (SEM) at ~10,000× magnification.

The relative group abundance (RGA) of total nannofossils in sediments was estimated by using a semiquantitative technique (e.g., roughly determining relative counts of nannofossils and other sediment particles within view fields on smear slides).

Calcareous nannofossils are built by delicate $CaCO_3$ elements. In deep-sea sediments, carbonate precipitation results in recrystallization of $CaCO_3$ elements of nannofossils, and they become larger or thicker, resulting in overgrowth of nannofossils. Carbonate dissolution leads nannofossils to be partly etched or totally dissolved. Both overgrowth and dissolution of nannofossils can be seen by using a microscope. Stages or degrees of overgrowth and dissolution can be estimated by a number of semiquantitative methods (Roth and Thierstein, 1972; Roth et al., 1975). In this study, nannofossil preservation was examined by means of LM, and the qualitative and quantitative estimation of degrees of dissolution and overgrowth was made using the computer program FossiList, as shown in Table 2.

In the Quaternary, a few *Gephyrocapsa* species are used as biostratigraphic markers. The method for separating and identifying *Gephyrocapsa* species follows Su (1996). Nannofossil datum ages used for Leg 168 are based on Su (1996) and on Shipboard Scientific Party (1997, Leg 167, California Margin). These datums are calibrated to the Cande and Kent (1995) time scale.

RESULTS OF BIOSTRATIGRAPHY

Biochronology for Pliocene and Quaternary Sediments

About 22 nannofossil species/taxa were recognized (Table 3). The nannofossil assemblage in the Juan de Fuca region is characterized by low species diversity and abundant cold-water species, such as *Coccolithus pelagicus, Gephyrocapsa muellerae, G. caribbeanica,* and abundant cosmopolitan species (e.g., *Emiliania huxleyi*). A few temperate-water species (*Helicosphaera carteri, H. sellii, Reticulofenestra asanoi,* etc.) are infrequent in hemipelagic layers. Tropical and subtropical species, such as the Pliocene marker species *Discoaster,* are absent. As a result, only a number of Quaternary nannofossil datums are useful for Leg 168.

During Leg 168, a number of Quaternary nannofossil events were suggested and used for the Quaternary sediment sequences in this

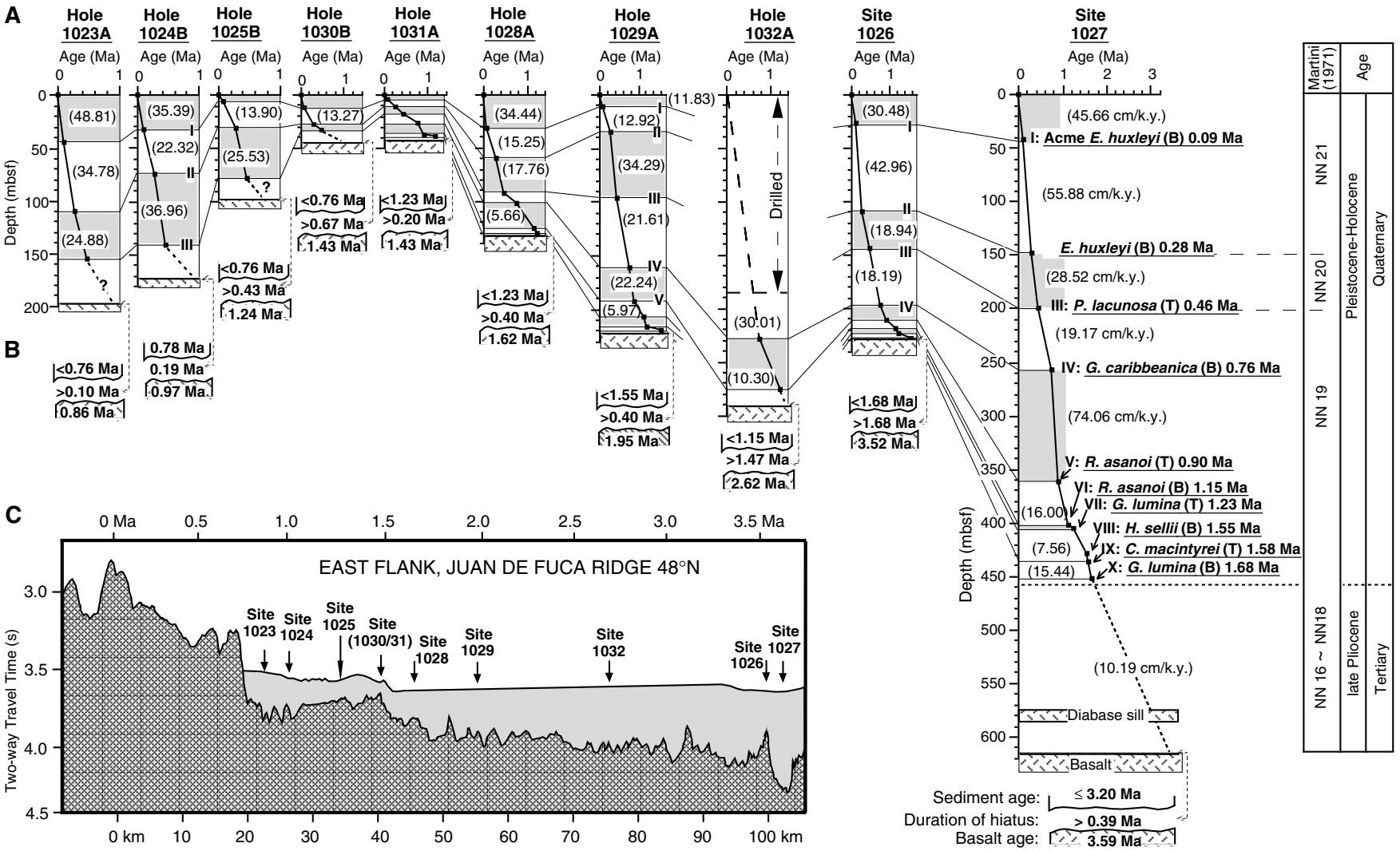

Figure 3. **A.** Biochronoloy and age models of Leg 168 sites, as well as correlation between the sites. Nannofossil zones (Martini, 1971) were also plotted as an age reference. Large variations in sedimentation rates between sites are probably due to topography in this area. **B.** The duration of sedimentation hiatus between initial sedimentation and basalt. **C.** Topography of basement in this area and detailed location of Leg 168 sites.

Table 2. Quaternary nannofossil events and their depths at Leg 168 sites.

Preservation stages	Definition
Dissolution	
1	No dissolution
2	>50% of specimens slightly etched, all taxa easily identified
3	>50% of specimens moderately etched, >50% taxa readily identified
4	>50% of specimens strongly etched and fragmented, low diversity
5	Almost all specimens strongly etched and fragmented, all species rare
6	Maximum dissolution; barren of coccoliths
Overgrowth	
1	No overgrowth
2	>50% of specimens slightly overgrown, all taxa easily identified
3	>50% of specimens moderately overgrown, >50% taxa readily identified
4	>50% of specimens strongly overgrown, low diversity
5	Almost all specimens strongly overgrown, all species rare
6	Maximum overgrowth, limestone, or calcareous debris; barren of identifiable coccoliths

Table 3. Coccolith species investigated in this study.

Genus *Emiliania* Hay and Mohler, in: Hay et al. 1967
E. huxleyi (Lohmann 1902) Hay and Mohler, in Hay et al. 1967
E. coronata Martini 1993

Genus *Gephyrocapsa* Kamptner 1943
G. caribbeanica Boudreaux and Hay 1967
G. lumina Bukry 1973
G. oceanica Kamptner 1943
G. margereli-muellerae group:
G. margereli Breheret 1978
G. muellerae Breheret 1978
Gephyrocapsa sp.V*
Gephyrocapsa spp. (small species)

Genus *Pseudoemiliania* Gartner 1968
P. lacunosa (Kamptner 1963) Gartner 1969

Genus *Reticulofenestra* Hay, Mohler and Wade 1966
R. asanoi Sato and Takayama 1991
R. minuta Roth 1970
R. minutula (Gartner 1967) Haq and Berggren 1978
R. perplexa (Burns 1975) Wise 1983
R. productella (Bukry 1975) Gallagher 1989

Genus *Calcidiscus* Kamptner 1950
C. leptoporus (Murray and Blackman 1898) Loeblich and Tappan 1978
C. macintyrei (Bukry and Bramlette 1969) Loeblich and Tappan 1978

Genus *Coccolithus* Schwarz 1894
C. pelagicus (Wallich 1877) Schiller 1930

Genus *Helicosphaera* Kamptner 1954
H. carteri (Wallich 1877) Kamptner 1954
H. sellii Bukry and Bramlette 1969

Genus *Pontosphaera* Lohmann 1902
Pontosphaera spp.

Genus *Rhabdosphaera* Haeckel 1894
R. claviger Murray and Blackman 1898

Genus *Syracosphaera* Lohmann 1902
S. pulchra Lohmann 1902
Syracosphaera spp.

area. In the postcruise study, these datums were further examined. The relative abundance of all these marker species at the 10 sites was determined. To give an example of these quantitative analyses, plots of a few marker species at Sites 1031 and 1027 are presented in Figure 4.

The determination of the base of *Emiliania huxleyi* was made by means of SEM to distinguish them from same-sized *Gephyrocapsa* species.

The base of acme *E. huxleyi* was determined by the distinct increase in relative abundance of this species and based on a correlation of this level among sites studied (Fig. 4).

Due to reworking, it is difficult to determine the last occurrence of *Gephyrocapsa lumina* (Fig. 4). Its last common occurrence was used, based on good agreements in correlation between sites (Table 4). The top of *Calcidiscus macintyrei* was determined in the same manner. The top of *G. caribbeanica* was selected for biostratigraphy during Leg 168, but it is not used in the present study because its last common occurrence varies largely from site to site (Fig. 4). Its last occurrence at Site 1027 is apparently much later than at other sites, due to major reworking from strong turbidite activity since the last 0.28 Ma, when a large number of very thick sand beds and sandy debris-flow deposits, with high sedimentation rates, accumulated in this buried valley (Fig. 3A, C).

During Leg 168 the determination of the top of *P. lacunosa* was difficult because this species was not recognized at Sites 1024 and 1025. In the shorebased study, samples from the lower parts of the sections at these two sites were examined by SEM, and this species was found to be present in these samples. When examined only by LM, these small varieties are difficult to separate from same-sized *Emiliania coronata* coccoliths, as well as from same-sized *Gephyrocapsa* coccoliths that have lost their bridges due to dissolution. Furthermore, they occur rarely in the upper Pleistocene sequences at these sites. Thus, the top of *P. lacunosa* was determined by examination with SEM after the cruise (Table 4).

As a result, the depths of these fossil events at all sites, as shown in Table 4, are more or less different from those in the *Initial Reports* of Leg 168 (Davis, Fisher, Firth, et al., 1997).

Because of the absence of upper Pliocene marker species, such as *Discoaster* species, a subdivision of the upper Pliocene sediment sequences was not made. On shipboard study, an age of younger than 3.5 Ma was estimated for the basal sediments at Site 1027, because the sediments do not contain large forms of *R. pseudoumbilicus* (>7 µm; LAD = 3.6 Ma). The nannofossil assemblage below Core 168-1027A-52X is characterized by the dominance of small- to medium-sized *Reticulofenestra* species: *R. minutula, R. minuta,* and *R. productella.* An abundance zone of these three species was recognized and can be correlated to the assemblage at Deep Ocean Drilling Program (DSDP) Leg 94, Site 610 from the northeast Atlantic (Fig. 5). Ages of Site 610 sediments were calculated based on geomagnetic data (Su, 1996), and are therefore reliable. Based on the correlation, an age of about 3.13 Ma was estimated for the base of the abundance zone, and an age of about 3.2 Ma was estimated for the basal sediment, the earliest sediment recovered by Leg 168.

Ages of all nannofossil samples at Site 1027 were calibrated by interpolation of the depths and ages of the nannofossil datums at this site (Table 4; Figs. 3, 5). The Pliocene/Pleistocene boundary was determined after Harland et al. (1990), who suggested an age of 1.64 Ma for this boundary. This data was further recalibrated to the Cande

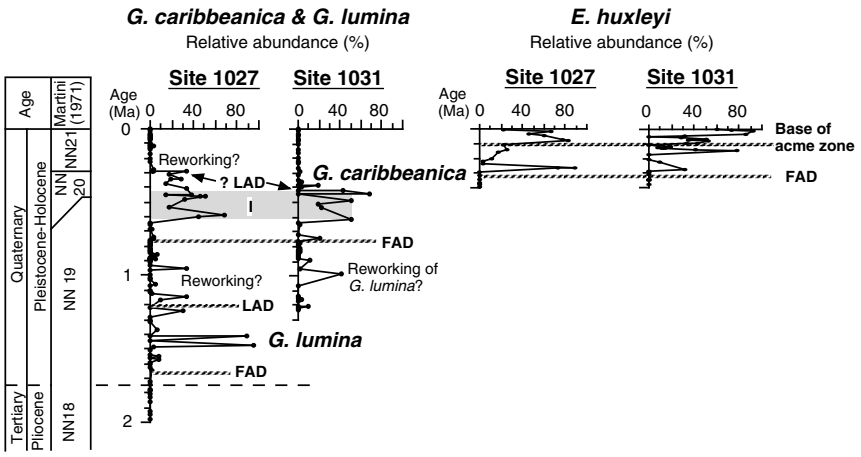

Figure 4. Plots of relative abundance and events of a few marker species at Sites 1027 and 1031.

Table 4. Definitions of coccolith preservation stages using the computer program FossiList.

Nannofossil events	Age (Ma)	Hole 1023A Depth	1024B Depth	1025B Depth	1030B Depth	1031A Depth	1028A Depth	1029A Depth	1032A Depth	1026B+C Depth*	1027B+C Depth*
B acme *E. huxleyi*	0.09	43.93	31.85	5.08	11.94	4.50	31.00	10.65		27.43	41.09
B *E. huxleyi*	0.28	110.02	74.25	31.49	27.85	10.67	59.97	35.19		109.06	147.27
T *P. lacunosa*	0.46	154.80	140.78	77.45	33.59	18.36	91.93	96.92		143.16	198.61
B *G. caribbeanica*	0.76					25.79	102.81	161.75	228.04	197.74	257.75
T *R. asanoi*	0.90					36.74		192.88		210.43	361.43
B *R. asanoi*	1.15					38.51	124.90	207.80		219.06	401.42
T *G. lumina*	1.23						129.77	216.55	276.43	223.96	404.43
T *H. sellii*	1.55									227.72	428.61
T *C. macintyrei*	1.58							219.55		228.70	436.41
B *G. lumina*	1.68										451.85

Notes: All depths are in meters below seafloor. * = Depth at Sites 1026 and 1027 are composed of depths from Holes B and C.

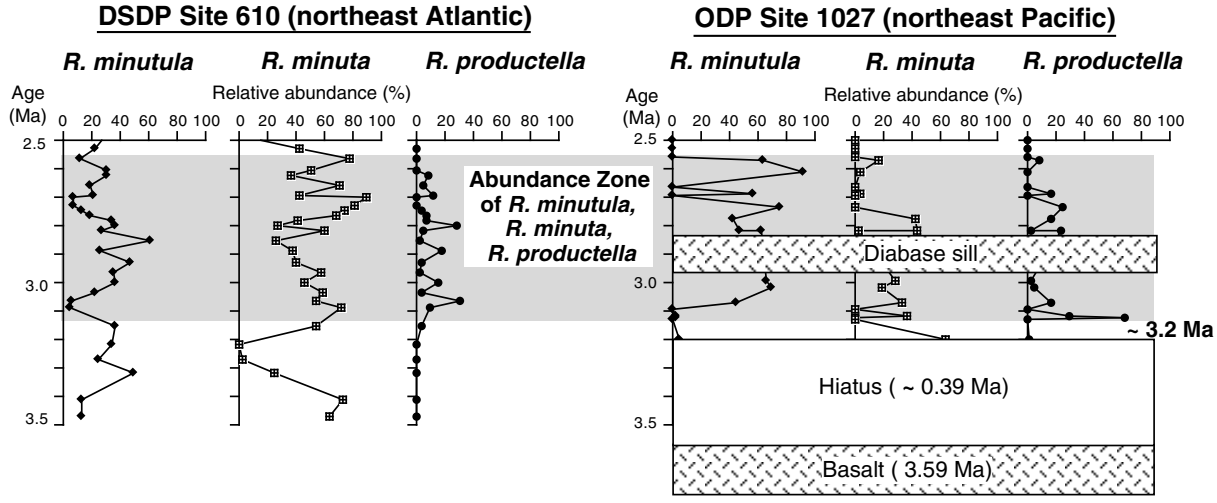

Figure 5. Correlation of relative abundance of small- to medium-sized *Reticulofenestra* species at ODP Site 1027 in the northeast Pacific and DSDP Site 610 in the northeast Atlantic.

and Kent (1995) time scale, and the correlated age for this boundary is 1.75 Ma. As a result, the Pliocene/Pleistocene boundary is placed at the depth 458.87 mbsf (1.746 Ma) at Site 1027.

Sedimentation Rates and Hiatuses

Based on nannofossil datums (Table 4), variations of sedimentation rates at the 10 sites were estimated (Fig. 3A). Generally, high values (>20 cm/k.y.) are commonly seen, varying largely from site to site. Since the last 0.09 Ma, for example, they vary from 4 cm/k.y. at Site 1031 on a crest, to 34.44 cm/k.y. at Site 1028 located on a valley nearby, and then to 45.66 cm/k.y. at the deepest valley Site 1027 (Fig. 3A, C), which leads to the suggestion that high values mostly resulted from strong turbiditic activity in these valleys. This agrees with lithologic observations of Leg 168, and more turbidite beds were found at these sites in valleys (Davis, Fisher, Firth, et al., 1997).

The sedimentation rate is lower during the late Pliocene than in the Quaternary. A value of 10.19 cm/k.y. was estimated for the upper Pliocene hemipelagic mud and carbon-rich mud deposits. Sedimentation rates increased with the beginning of the Quaternary, and numbers of turbidites beds occur in the Quaternary sequences (Figs. 6–8). These turbidite sediments are supplied from glacial sources along the continental margin (Davis et al., 1992); increased sedimentation rates in the Quaternary therefore imply that the amount of the input of turbiditic materials into this region is larger than in the late Pliocene, due to intensified glacial/interglacial climate changes since the Quaternary.

Variations in sedimentation rate during the Quaternary were also noted. In the early period of the Quaternary (1.75– 0.90 Ma), sedimentation rates in this area are relatively low, varying from 7.56 to 16.00 cm/k.y. at Site 1027 (Fig. 3A). Hemipelagic mud layers that formed in this period were recovered not only at Site 1027, but also from the lower sections at Sites 1031, 1028, 1029, 1032, and 1026. Since the last 0.46 Ma, sedimentation rates increased distinctly, showing high values (>30 cm/k.y) at most of the sites studied. This is consistent with results of shipboard lithostratigraphic studies which recognized a large number of thick sand beds of late Quaternary age at these sites (Davis, Fisher, Firth, et al., 1997; Figs. 6–8).

Based on geomagnetic data obtained during Leg 168 and nannofossil data in this study, a comparison of ages of basal sediments and basements at all Leg 168 sites was made (Fig. 3B). The ages of basal sediments are consistent with their basement ages, although they are much younger than the later sediments, indicating a hiatus between the onset of sedimentation and the crustal formation in this young seafloor-spreading area. The shortest hiatus (~0.1 Ma) was observed at Site 1023 and is located about 23 km from the axis of the Juan de Fuca Ridge. The significant hiatuses are >1.47 Ma at Site 1032 and >1.68 Ma at Site 1026. An increase in the duration of these hiatuses from the western sites to the eastern sites was noted (Fig. 3B). Sedimentation hiatuses in the studied area are probably due to strong bottom currents or inclined seafloor in the early stages of sedimentation. For example, the duration of the hiatus at Site 1026 is estimated to be >1.68 Ma. According to shipboard observations (Davis, Fisher, Firth, et al., 1997), in the deepest strata from Hole 1026C, color bands and *Zoophycos* traces are inclined at apparent dip angles of 15°–20°, and there are also several offsets along small normal faults, indicating the early stages of sedimentation occurred on a steeply inclined seafloor.

OBSERVATIONS AND DISCUSSIONS ON POSTDEPOSITIONAL VARIATIONS OF NANNOFOSSILS

Figures 6–8 show plots of nannofossil RGA and nannofossil overgrowth and dissolution stages at each Leg 168 site with the exception of Sites 1024 and 1032, because nannofossil records at Site 1024 are similar to those at Site 1023, and sediments above 184.5 mbsf at Site 1032 were drilled.

In these figures, lithostratigraphic data, geochemical data (carbonate content, and calcium and pH of pore water), and data from temperature measurements, which were obtained by shipboard studies, were plotted for comparison.

In addition, during Leg 168, 10 individual sites were grouped into three operational "super sites" according to geographic area, represented process, and primary objectives. They are (1) Hydrothermal Transition Transect (Sites 1023, 1024, and 1025), (2) Buried Basement Transect (Sites 1028, 1029, 1030, 1031, and 1032), and (3) Rough Basement Transect (Sites 1026 and 1027). Sites presented in Figures 6–8 are also arranged in this way (e.g., Fig. 8 gives the data from the Rough Basement Transect Sites 1026 and 1027).

Effects of Turbidites on Nannofossil Records

According to shipboard lithostratigraphic studies (Davis, Fisher, Firth, et al., 1997), sediments recovered at most sites were divided into three subunits or units: Unit II, which is comprised of hemipelagic mud and carbonate-rich mud; Subunit IB, which contains interbedded silt turbidites and hemipelagic mud; and Subunit IA, which is composed of sand turbidites, silt turbidites, and hemipelagic mud. These sites are Sites 1023–1029 and 1032, which are located in valleys on the eastern flank of the Juan de Fuca Ridge (Fig. 3C) and therefore received more turbiditic materials.

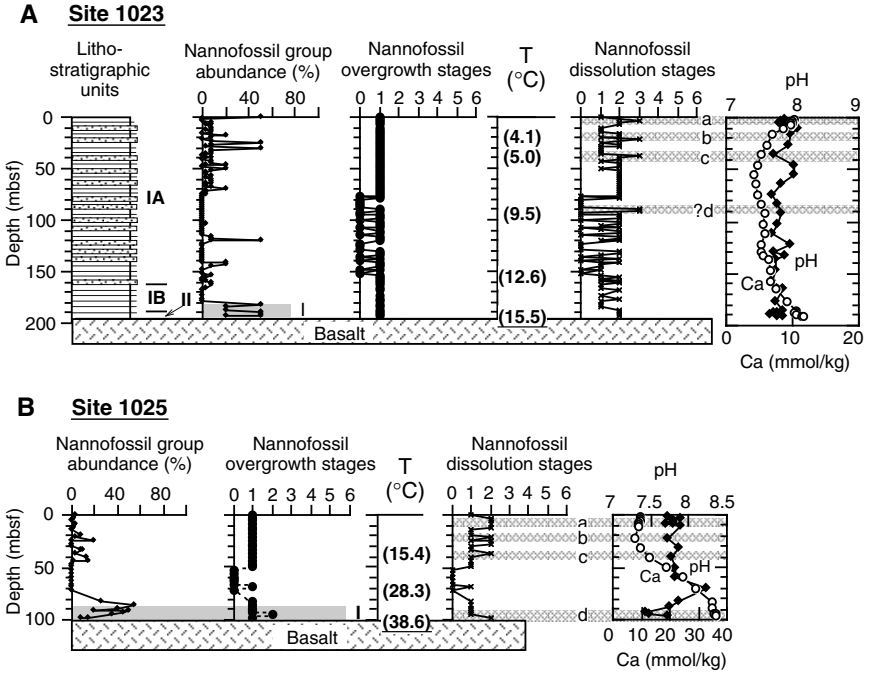

Figure 6. Plots of degrees of nannofossil preservation along Hydrothermal Transition Transect sites. **A.** Site 1023. **B.** Site 1025. Reference data of lithostratigraphic units; profiles of carbonate content, calcium, and pH; and data from temperature measurements are from Davis, Fisher, Firth, et al. (1997).

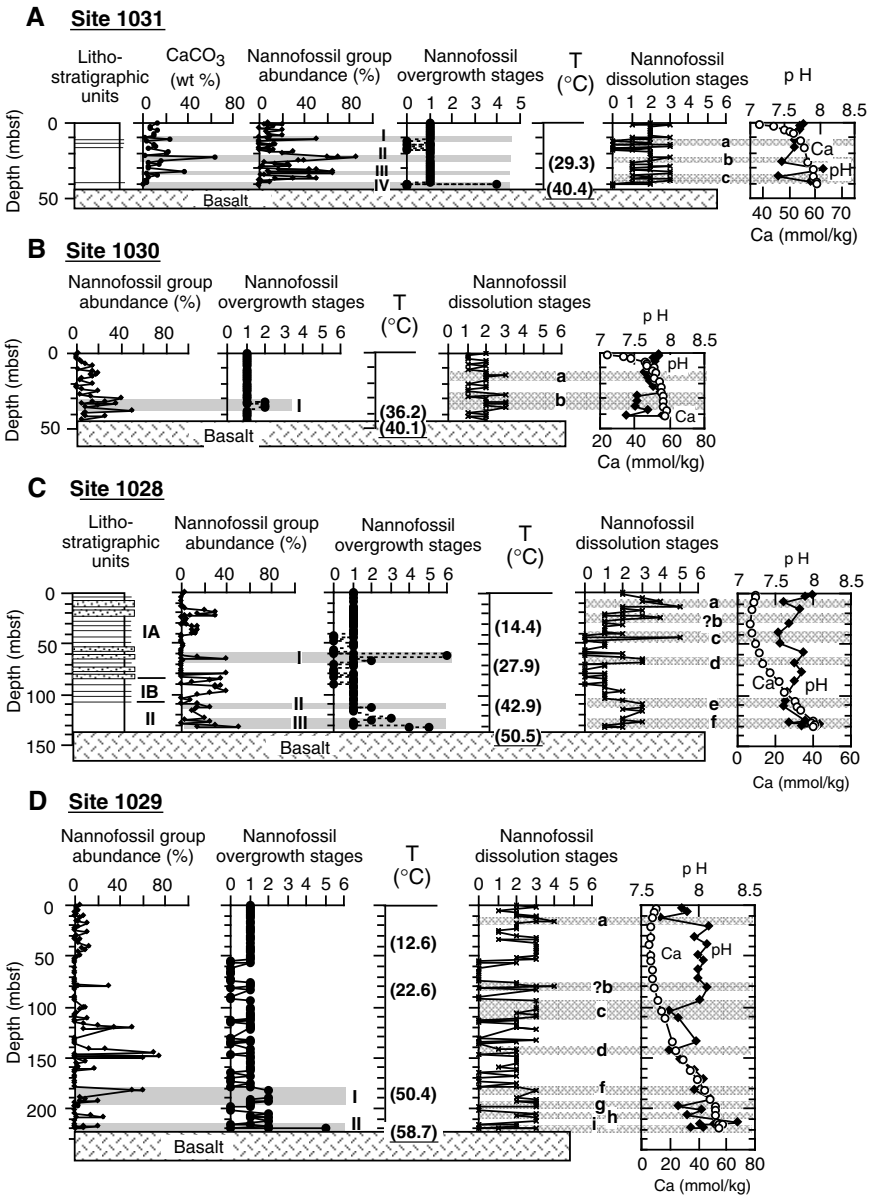

Figure 7. Plots of degrees of nannofossil preservation along Buried Basement Transect sites. **A.** Site 1030. **B.** Site 1031. **C.** Site 1028. **D.** Site 1029. Reference data of lithostratigraphic units; profiles of carbonate content, calcium, and pH; and data from temperature measurements are from Davis, Fisher, Firth, et al. (1997).

Downhole variations in nannofossil RGA were noted at Sites 1023, 1028, and 1027 (Figs. 6A, 7C, 8B). High values (>40%) of nannofossil RGA occur mainly within Unit II and Subunit IB, and low values (<30%) were found within Subunit IA. Subunit IA at Sites 1027 and 1026 contains numbers of thick sand turbidites, where nannofossil RGA are commonly lower than 1% (Fig. 8B). The sedimentation variations at these sites suggest an increase in input of turbiditic materials from Unit II to Subunit IA. An upward reduction of nannofossil RGA in correlation with an increase of turbiditic materials at these sites can be clearly seen from Figures 6–8.

What is the Effect of These Turbidite Materials on Nannofossil Records?

Site 1031 is located on a ridge crest with thin (~40 m) sediment cover that is composed of hemipelagic mud with rare silt interbeds, being less affected by turbidites. Values of nannofossil RGA at Site 1031 range commonly from 20% to 80%, showing highest values among all Leg 168 sites. Based on our biostratigraphic results, sediments above 18 mbsf at Site 1031 and those above 200 mbsf at Site 1027 are formed during the same period after 0.46 Ma (Fig. 3A). In this time interval, nannofossil RGA values (10%–20%) at Site 1031 are >10 times higher than those (<1%) at Site 1027.

The above evidence suggests that variations in nannofossil RGA through time and among sites in the Juan de Fuca Ridge are largely affected by dilution of turbiditic materials and thus do not reflect the real variations in production of this group of microfossils.

Downhole Variations of Nannofossil RGA and Carbonate Content

Figures 7A and 8B illustrate downhole variations in nannofossil RGA and in carbonate content of sediments at Sites 1031 and 1027.

A correlation between these two different curves suggests they have similar downhole variation patterns. In addition, this correlation

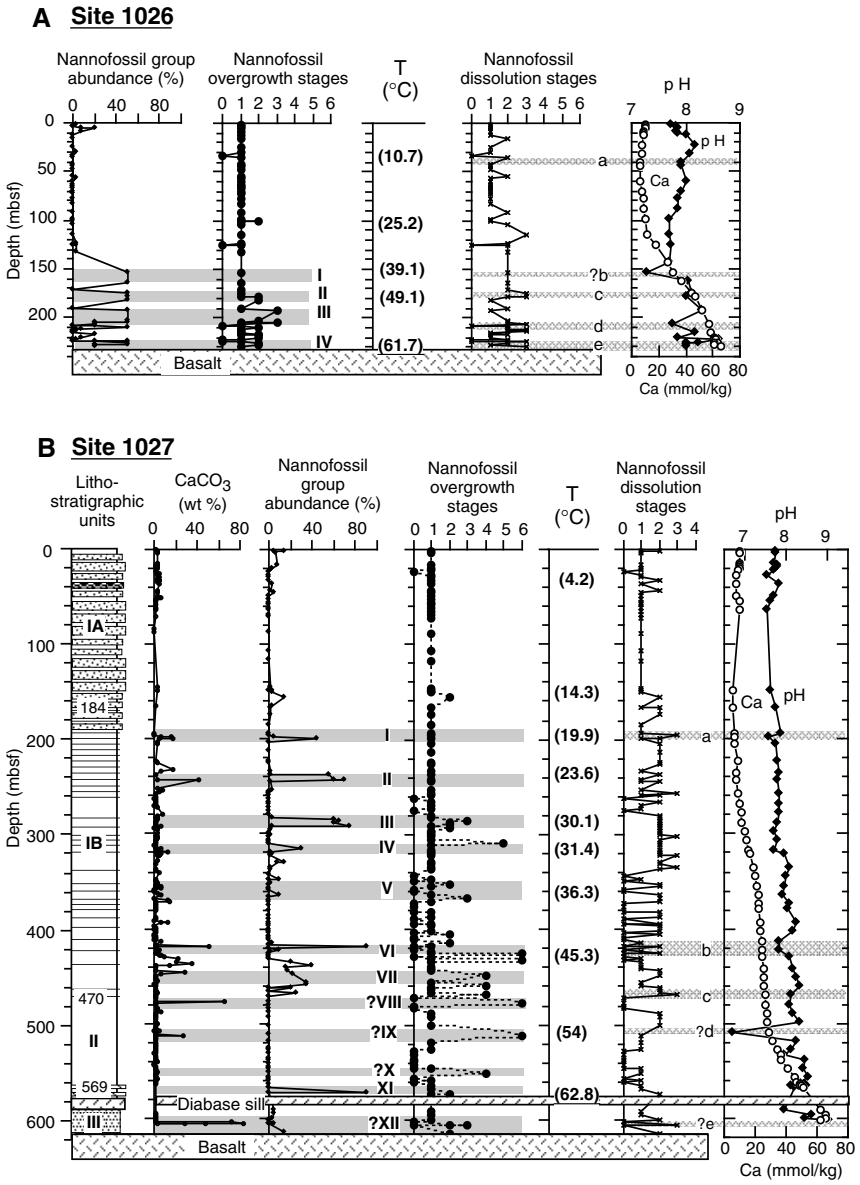

Figure 8. Plots of degrees of nannofossil preservation along Rough Basement Transect sites. **A.** Site 1026. **B.** Site 1027. Reference data of lithostratigraphic units; profiles of carbonate content, calcium, and pH; and data from temperature measurements are from Davis, Fisher, Firth, et al. (1997).

also suggests that the method of semiquantitative determination of nannofossil RGA produced reliable nannofossil data.

In the lower part of the section at Site 1027, several $CaCO_3$ peaks are distinct (e.g., peaks VIII, IX, and XII; Fig. 8B), whereas the nannofossil RGA curve indicates that it is barren of nannofossils. From the records of nannofossil overgrowth we can see that the maximum overgrowth (Stage 6) of nannofossils occurred in these layers. In Stage 6, nannofossils have changed into calcareous debris, and no nannofossil species can be identified; thus the RGA values are low. Therefore, this discrepancy between records of nannofossil RGA and carbonate content is seen as a result of hydrothermal alteration.

In addition, values of nannofossil RGA are generally higher than those of $CaCO_3$. At Site 1031, the nannofossil RGA value at peak II is 80%, whereas the value of carbonate content is 60% (Fig. 7A). This is mostly due to differences in sampling. Most nannofossil samples were carefully collected from thin- and fine-grained hemipelagic layers that are more rich in nannofossils, whereas the data from a $CaCO_3$ sample is the mean value for about a 2-cm sediment interval, which may contain turbidite layers, and the carbonate content in these layers is diluted.

Overgrowth of Nannofossils

Definitions of nannofossil preservation stages are given in Table 4. A number of Leg 168 samples do not contain any nannofossils, and no determination of nannofossil preservation was made. The "0" stage is added for these samples in plots of overgrowth and dissolution stages (Figs. 6–8).

Along the Hydrothermal Transition Transect sites (Fig. 6), only one sediment sample near basement at Site 1025 contains slightly overgrown (Stage 2) nannofossils.

Overgrown nannofossils were found in all Buried Basement Transect sites, mostly from the lowest sediments lying directly on basements (Fig. 7). Exceptionally, slightly to very strongly overgrown nannofossils were also seen from a few samples in the interval from 61.1 to 67.45 mbsf at Site 1028.

Along the Rough Basement Transect sites (Fig. 8), slightly to strongly overgrown nannofossils were observed in a number of samples below 1.75 mbsf at Site 1026 and below 280 mbsf at Site 1027; above these depths only two samples contain slightly overgrown nannofossils. In a number of samples (e.g., peaks IV, VI, VIII, IX, X, and XI at Site 1027), nannofossils were changed into calcareous debris, so that nannofossil RGA values are very low. Among all Leg 168 sites, Site 1027 contains the most abundant layers with overgrown nannofossils and the longest interval (>300 m) in which hydrothermal alteration observed.

In general, there is a gradual increase in overgrowth degrees and numbers of sediment layers from the western sites towards the eastern sites. This phenomenon suggests a correlation with the heat flow profile along the eastern flank of the Juan de Fuca Ridge. Now it is of considerable interest to know if hydrothermal circulation in this area affects the preservation of nannofossils and, if so, how this is accomplished.

Normally, we know that the overgrowth of nannofossils in sediments, either by recrystallization or carbonate precipitation, is mainly controlled by the variation in composition of pore fluids in sediments. Our knowledge about the effect of hydrothermal alteration on diagenesis is very limited. Mao and Wise (1994) found that nannofossils preserved in sediments of the Middle Valley of the Juan de Fuca Ridge were strongly dissolved due to hydrothermal activity with high temperatures (65°–>200°C).

Does hydrothermal alteration, and especially low-temperature alteration, also affect the recrystallization of nannofossils? Now we need to examine various possible control factors one by one.

Temperature and Heat Flow

Among the western sites (Fig. 6), overgrown nannofossils were seen only in the basal sediments at Site 1025 (basement temperature 38.4°C; heat flow 443 mW/m^2). Site 1023 (15.5°C; 84 mW/m^2) does not contain overgrown nannofossils. Along Buried Basement Transect sites, all basement temperatures are higher than 40°C, and nearly all samples from the basal sediments contain overgrown nannofossils. The basement temperature at Site 1031 (40.4°C) is somewhat higher than that at Site 1025 (38.4°C), but its heat flow (1087 mW/m^2) is much higher than that at Site 1025, and the overgrowth degree of nannofossils at Site 1031 is stronger (Stage 4) than that at Site 1025 (Stage 2). On the other hand, the nannofossil overgrowth stage at Site 1031 is weaker than that at Site 1029 (Stage 5). These facts suggest that temperature and heat flow play an important role in recrystallization of nannofossils, and that they often show a combined effect. The comparison of these data at Sites 1023 and 1025 suggests that the hydrothermal alteration of nannofossils occurs above a certain temperature or heat flow value; the lowest temperature is probably 30°C, according to the highest level of overgrowth at Site 1027.

There is a general decreasing upward trend in degrees and occurrences of overgrowth of nannofossils at Sites 1027, 1026, 1029, and 1028, in correlation with the decrease in temperature and heat flow in sediments (Figs. 6–8). This indicates that the hydrothermal alteration of nannofossils decreases in correlation with the reduction of heat flow and temperature.

Furthermore, we noted that the upward decrease in degree and occurrence of overgrowth of nannofossils at Site 1027 is more gradual than at other sites. In this case, the thermal gradient in sediments should be considered. At Site 1027, the thermal gradient (0.103°C/m) is lowest among all sites, which leads to the gradual reduction of heat flow and temperature at this site.

Variation in Composition of Pore Water

It would be beyond the scope of this study to discuss this topic in detail. Only profiles of calcium and pH were therefore selected for comparison.

From Figures 6–8 we saw that an increase of calcium can be correlated to an increase in nannofossil RGA value and carbonate content, and vice versa. Samples that contain overgrown nannofossils occur commonly within the intervals where calcium increased and pH units were high.

Hemipelagic Layers

Layers that contain overgrown nannofossils mainly occur in the lower part of the sections at Sites 1025, 1028, 1029, 1026, and 1027, because they are hemipelagic layers (e.g., peak I at Site 1025; peak II at Site 1029; peaks III, VI, and VII at Site 1027; Figs. 6–8).

Why does calcite overgrowth of nannofossils occur in hemipelagic layers rather than in turbidite beds in which nannofossils are very few or absent? One possibility is that abundant nannofossils, probably together with planktonic foraminifers that also occur commonly in these hemipelagic layers, provide calcite materials for the reactions of hydrothermal fluids with sediments.

Dissolution of Nannofossils

Dissolution of nannofossils was seen in all Leg 168 sites, showing a variety of stages between sites and downhole intervals. Generally, slightly etched to moderately dissolved nannofossils were found at the Hydrothermal Transition Transect sites and the Rough Basement Transect sites. Moderately dissolved to very strongly dissolved nannofossils were observed among the Buried Basement Transect sites (Figs. 6–8).

The composition of coccolith skeletons is pure calcium (with low Mg); coccoliths are therefore significantly resistant to dissolution (Bukry, 1971a; Cook and Egbert, 1983; Steinmetz, 1994). Degrees of dissolution of biogenetic carbonate particles in sediment are controlled by a number of factors, including (1) selective dissolution, (2) water depth and carbonate cycles, and (3) variation in composition of pore fluids in sediments. A brief discussion on these factors is given below.

1. Selective dissolution exists between nannofossil species with different ultrastructures. Nannofossils found in Leg 168 sediments are mainly placoliths (Table 3), such as *Gephyrocapsa, Emiliania, Coccolithus,* and *Reticulofenestra,* which are the taxa resistant to dissolution. Dissolution degrees presented in Figures 6–8 are not due to selective dissolution.
2. The calcite compensation depth (CCD) and the lysocline are important for the dissolution of nannofossils. The CCD lies at depths about 3300 m along margins of the Pacific basin, and the lysocline is found usually a few hundred meters above the CCD. Water depths of all Leg 168 sites are about 2574–2679 m (Table 1), far above the CCD and the lysocline. Furthermore, if a strong dissolution layer is induced by the lysocline, this layer should occur in a certain time period and can be correlated between our sites. Such layers are not seen at Leg 168 sites. Therefore, the controls of the CCD and the lysocline can be ruled out.
3. The variation in composition of pore fluids in sediments in situ might be the main cause for our moderate to strong dissolution records.

For this reason, we selected pH data from shipboard pore-water geochemical studies for comparison (Figs. 6–8). These irregular nannofossil dissolution records can be well correlated to the pH records at each site. In the most cases, the dissolution peaks of nannofossils parallel low pH values (peaks a and c at Sites 1023 and 1025; peaks a–c at Site 1031; peaks a–b at Site 1030; peaks a–f at Site 1028; peaks a–i at Site 1029; and peaks a–e at Sites 1026 and 1027) and vice versa. A few peaks are not correlated, because of different sample intervals of these two sets of data (e.g., nannofossil

peak "?b" at 30 mbsf at Site 1028, which is located just within the interval of two samples of pH data).

The correlation between nannofossil dissolution and pH data indicates that nannofossils are very sensitive to pH variations in sediment columns. The reduction of pH in sediments will result in dissolution of nannofossils.

Moderately dissolved nannofossils through the sediment sections at Sites 1031 and 1032 are further connected to the pore-water upward flows at these two sites. The upward flow at Site 1031 was faster than that at Site 1030 (Davis, Fisher, Firth, et al., 1997); as a result, more layers containing moderately dissolved nannofossils are found at Site 1031.

Now we obtain a detailed correlation between nannofossil dissolution and variations in pore water. The variation in pH values is a result of complicated variations in concentrations of various elements. Based on studies of fluid geochemistry during Leg 168, pore fluids are affected by a number of processes, including their reactions with rocks in basement and overlying sediments, which involves numerous diagenesis processes and hydrothermal activity (Davis, Fisher, Firth, et al., 1997). This study, however, is still unable to discuss the mechanisms of pore fluids on nannofossil dissolution in detail. Results from postcruise geochemistry studies would give more details about these changes.

CONCLUSION

The nannofossil assemblages in the studied area are characterized by low species diversity and by the dominance of cold-water forms or cosmopolitan species.

A detailed biochronology for Quaternary sediments on the eastern flank of the Juan de Fuca Ridge was obtained, providing basic knowledge for various studies related to Leg 168 and to the area of the Juan de Fuca Ridge. The upper Pliocene sequences at Site 1027 do not contain any upper Pliocene marker species, such as *Discoaster* species. An age of 3.2 Ma or younger was estimated for these sediments based on results from analyzing nannofossil assemblages. Based on the resolved biochronology, sedimentation rates of sediment sequences at these 10 sites and their variations were determined. A sedimentation hiatus between basal sediments and basements in this young seafloor region was observed.

A number of results suggest that variations in nannofossil RGA in the Juan de Fuca Ridge, affected by dilution of turbiditic materials, do not reflect the real variation in production of this group of microfossils.

This study found that calcite overgrowth of nannofossils is controlled by temperature, heat flow, thermal gradient in sediments, and the variation in composition of pore water, as well as the supply of calcite materials in sediments. These results provide a detailed knowledge about the effects of low-temperature hydrothermal alteration on diagenesis of nannofossils.

Nannofossils are very sensitive to variations of pore-water pH in sediments: a reduction in pH resulted in the dissolution of nannofossils. The dissolution of nannofossils at Sites 1031 and 1032 were also directly affected by the pore-water upward flows at these two sites.

A few records of nannofossil preservation suggest that the effects of hydrothermal activity on diagenesis of nannofossils might involve more complicated processes and mechanisms that we do not yet understand.

ACKNOWLEDGMENTS

We are grateful to the crew and scientists on the cruise of Leg 168, and the Curator of the Ocean Drilling Program, for obtaining and sharing samples and data of this leg. This project is financially supported by the German Science Foundation (DFG Grant Th 200/28-1) during the Leg 168 cruise and thereafter. The authors thank reviewer Dr. W. Wei and an anonymous reviewer whose comments improved the manuscript.

REFERENCES

Baker, E.T., Massoth, G.J., and Feely, R.A., 1987. Cataclysmic hydrothermal venting on the Juan de Fuca Ridge. *Nature,* 329:149–151.

Bukry, D., 1971a. Cenozoic calcareous nannofossils from the Pacific Ocean. *Trans. San Diego Soc. Nat. Hist.,* 16:303–327.

————, 1971b. Coccolith stratigraphy, Leg 8, Deep Sea Drilling Project. *In* Tracey, J.I., Jr., et al., *Init. Repts. DSDP,* 8: Washington (U.S. Govt. Printing Office), 791-807.

————, 1973. Calcareous nannofossils from cores recovered during Leg 18, Deep Sea Drilling Project: biostratigraphy and preservations of diagenesis. *In* Kulm, L.D., von Huene, R., et al., *Init. Repts. DSDP,* 18: Washington (U.S. Govt. Printing Office), 569–615.

————, 1981. Pacific coast coccolith stratigraphy between Point Conception and Cabo Corrientes, Deep Sea Drilling Project Leg 63. *In* Yeats, R.S., Haq, B.U., et al., *Init. Repts. DSDP,* 63: Washington (U.S. Govt. Printing Office), 445–471.

Bukry, D., and Bramlette, M.N., 1970. Coccolith age and determinations Leg 5, Deep Sea Drilling Project. *In* McManus, D.A., and Burns, R.E., et al., *Init. Repts. DSDP,* 5: Washington (U.S. Govt. Printing Office), 487–494.

Cande, S.C., and Kent, D.V., 1995. Revised calibration of the geomagnetic polarity timescale for the Late Cretaceous and Cenozoic. *J. Geophys. Res.,* 100:6093–6095.

Cook, H.E.,and Egbert, R.M., 1983. Diagenesis of deep-sea carbonates. *In* Larsen, G., and Chillingar, G.V. (Eds.), *Diagenesis in Sediments and Sedimentary Rocks:* Amsterdam (Elsevier), 213–288.

Davis, E.E., Chapman, D.S., Mottl, M.J., Bentkowski, W.J., Dadey, K., Forster, C., Harris, R., Nagihara, S., Rohr, K., Wheat, G., and Whiticar, M., 1992. FlankFlux: an experiment to study the nature of hydrothermal circulation in young oceanic crust. *Can. J. Earth Sci.,* 29:925–952.

Davis, E.E., and Currie, R.G., 1993. Geophysical observations of the northern Juan de Fuca Ridge system: lessons in sea-floor spreading. *Can. J. Earth Sci.,* 30:278–300.

Davis, E.E., and Fisher, A.T., 1994. On the nature and consequences of hydrothermal circulation in the Middle Valley sedimented rift: inferences from geophysical and geochemical observations, Leg 139. *In* Mottl, M.J., Davis, E.E., Fisher, A.T., and Slack, J.F. (Eds.), *Proc. ODP, Sci. Results,* 139: College Station, TX (Ocean Drilling Program), 695–717.

Davis, E.E., Fisher, A.T., Firth, J.V., et al., 1997. *Proc. ODP, Init. Repts.,* 168: College Station, TX (Ocean Drilling Program).

Davis, E.E., Mottl, M.J., Fisher, A.T., et al., 1992. *Proc. ODP, Init. Repts.,* 139: College Station, TX (Ocean Drilling Program).

Gartner, S., 1970. Coccolith age determinations Leg 5, Deep Sea Drilling Project. *In* McManus, D.A., Burns, R.E., et al., *Init. Repts. DSDP,* 5: Washington (U.S. Govt. Printing Office), 495–500.

Ginster, U., Mottl, M.J., and von Herzen, R.P., 1994. Heat flux from black smokers on the Endeavour and Cleft segments, Juan de Fuca Ridge. *J. Geophys. Res.,* 99:4937–4950.

Haq, B., and Lipps, J.H., 1971. Calcareous nannofossils. *In* Tracey, J.I., Jr., Sutton, G.H., et al., *Init. Repts. DSDP,* 8: Washington (U.S. Govt. Printing Office), 777–790.

Harland, W.B., Armstrong, R.L., Cox, A.V., Craig, L.E., Smith, A.G., and Smith, D.G., 1990. *A Geologic Time Scale 1989:* Cambridge (Cambridge Univ. Press).

Hay, W.W., 1971. Preliminary dating by fossil calcareous nannoplankton, Deep Sea Drilling Project, Leg 8. *In* McManus, D.A., Burns, R.E., et al., *Init. Repts. DSDP,* 5: Washington (U.S. Govt. Printing Office), 809–818.

Lister, C.R.B., 1970. Heat flow west of the Juan de Fuca Ridge. *J. Geophys. Res.,* 75:2648–2654.

Mao, S., and Wise, S.W., Jr., 1994. Late Quaternary calcareous nannofossils from the sedimented Middle Valley of the Juan de Fuca Ridge, Leg 139. *In* Mottl, M.J., Davis, E.E., Fisher, A.T., and Slack, J.F. (Eds.), *Proc. ODP, Sci. Results,* 139: College Station, TX (Ocean Drilling Program), 59–76.

Martini, E., 1971. Standard Tertiary and Quaternary calcareous nannoplankton zonation. *In* Farinacci, A. (Ed.), *Proc. 2nd Int. Conf. Planktonic Microfossils Roma:* Rome (Ed. Tecnosci.), 2:739–785.

Roth, P.H., and Thierstein, H., 1972. Calcareous nannoplankton: Leg 14 of the Deep Sea Drilling Project. *In* Hayes, D.E., Pimm, A.C., et al., *Init. Repts. DSDP,* 14: Washington (U.S. Govt. Printing Office), 421–485.

Roth, P.H., Wise, S.W., and Thierstein, H.R., 1975. Early chalk diagenesis and lithification: sedimentological applications of paleontological approaches. *9th Int. Sedimentol. Congr.,* 7:187–199.

Shipboard Scientific Party, 1997. Explanatory notes. *In* Lyle, M., Koizumi, I., Richter, C., et al., *Proc. ODP, Init. Repts.,*167: College Station, TX (Ocean Drilling Program), 15–39.

Steinmetz, J., 1994. Sedimentation of coccolithophores. *In* Winter, A., and Siesser, W.G. (Eds.), *Coccolithophores:* Cambridge (Cambridge Univ. Press), 179–197.

Su, X., 1996. Development of Late Tertiary and Quaternary coccolith assemblages in the Northeast Atlantic. *GEOMAR Rep.,* 48.

Vine, F.J., and Wilson, J.T., 1995. Magnetic anomalies over a young oceanic ridge off Vancouver Island. *Science,* 150:485–489.

Wise, S.W., Jr., 1973. Calcareous nannofossils from cores recovered during Leg 18, Deep Sea Drilling Project: biostratigraphy and observations of diagenesis. *In* Kulm, L.D., von Huene, R., et al., *Init. Repts. DSDP,* 18: Washington (U.S. Govt. Printing Office), 569–615.

Worsley, T.R., 1973. Calcareous nannofossils: Leg 19 of the Deep Sea Drilling Project. *In* Creager, J.S., Scholl, D.W., et al., *Init. Repts. DSDP,* 19: Washington (U.S. Govt. Printing Office), 741–750.

Date of initial receipt: 11 December 1998
Date of acceptance: 27 June 1999
Ms 168SR-015